Bioorganic Chemistry 88 (2019) 102962

Contents lists available at ScienceDirect

Bioorganic Chemistry

journal homepage: www.elsevier.com/locate/bioorg

Novel 9-(2-(1-arylethylidene)hydrazinyl)acridine derivatives: Target Topoisomerase 1 and growth inhibition of HeLa cancer cells

Md Rafi Haider[a], Kamal Ahmad[a], Nadeem Siddiqui[a], Zulphikar Ali[a], Md Jawaid Akhtar[a,d], Neeraj Fuloria[b], Shivkanya Fuloria[b], Manickam Ravichandran[c], M. Shahar Yar[a,*]

[a] Department of Pharmaceutical Chemistry, School of Pharmaceutical Education and Research (SPER), Jamia Hamdard, Hamdard Nagar, New Delhi 110062, India
[b] Department of Pharmaceutical Chemistry, Faculty of Pharmacy, AIMST University, Semeling Campus, Jalan Bedong-Semeling, Bedong, Kedah Darul Aman 08100, Malaysia
[c] Faculty of Applied Science, AIMST University, Semeling Campus, Jalan Bedong-Semeling, Bedong, Kedah Darul Aman 08100, Malaysia
[d] School of Pharmacy, Bharat Institute of Technology, NH 58, Partapur Bypass, Meerut 250103, India

ARTICLE INFO

Keywords:
Anticancer
Topoisomerase1
Antioxidant
Docking
Acridine

ABSTRACT

A series of 9-(2-(1-arylethylidene)hydrazinyl)acridine and its analogs were designed, synthesized and evaluated for biological activities. Various biochemical assays were performed to determine the free radical scavenging capacity of synthesized compounds (**4a–4j**). Anticancer activity of these compounds was assessed against two different human cancer cell lines viz cervical cancer cells (HeLa) and liver cancer cells (HepG2) as well as normal human embryonic kidney cell line (HEK 293). Compounds **4b**, **4d** and **4e** showed potential anti-proliferative effects on HeLa cells. Based on results obtained from antioxidant and cytotoxicity studies, **4b**, **4d** and **4e** were further studied in detail for different biological activities. **4b**, **4d** and **4e** reduced the cell growth, inhibited metastatic activity and declined the potential of cell migration in HeLa cell lines. Topoisomerase1 (Top1) treated with compounds **4b**, **4d** and **4e** exhibited inhibition of Top1 and prevented DNA replication. Molecular docking results validate that interaction of compounds **4b**, **4d** and **4e** with Top1-DNA complex, which might be accountable for their inhibitory effects. Further it was concluded that compounds **4b**, **4d** and **4e** arrests the cells at S phase and consequently induces cell death through DNA damage in HeLa cells.

1. Introduction

Cancer is one of the major health issues globally with several clinical challenges which increase every year cumulatively [1]. Cancer is characterized by uncontrolled growth of cells which invades to other parts of the body and considered as most deadly health crisis next to cardiovascular diseases [2]. Till date, several cytotoxic drugs have already been developed to fight cancer. However, most of these drugs have lesser therapeutic efficacy and are associated with many undesirable side effects [3]. Hence, constant search for safer new chemical entities with substantial anticancer activity, and identification of efficient cellular targets are needed for the effective cancer treatment [4,5]. From literature survey, it was evident Topoisomerase 1 (Top1) express itself constitutively in several forms of cancer (lymphoma, breast, leukemia, lung, ovarian and prostate) and have vital roles in cancer cell growth, survival and development [6–9]. Top1 is an enzyme essential for DNA replication and transcription. During cellular processes of replication or transcription, double stranded DNA acquires significant degree of both positive and negative supercoiling [10,11]. Top1 resolves the topological problems arising due to supercoiling and allow effective replication and transcription [11]. Top1 imparts its action with the help of a nucleophilic tyrosine residue that nicks a single strand of the DNA and allows “controlled rotation” of the DNA around the other strand, thus relax the double helix of DNA [10–12]. Since, Top1 is especially expressed in the S-phase of the cell cycle and an increased level has been proven in several solid human tumors, it has long been acknowledged as an effective target for the design and development of cancer chemotherapeutics [10,12]. Use of some of the established Top1 inhibitors include Camptothecin, Irinotecan, Topotecan, Rubitecan, indenoisoquinolines depicted in Fig. 1, remains limited due to side effects, high toxicity and emerging drug resistance [13–16]. Therefore, there is necessity to find a novel drug that can reveal promising anti-proliferative activity with least toxicity and lower side effects.

In an effort to find active anticancer agents targeting Top1, several constructive works have been made on the improvement of heterocyclic

* Corresponding author.
E-mail address: yarmsy@rediffmail.com (M.S. Yar).

https://doi.org/10.1016/j.bioorg.2019.102962
Received 7 March 2019; Received in revised form 21 April 2019; Accepted 28 April 2019
Available online 03 May 2019

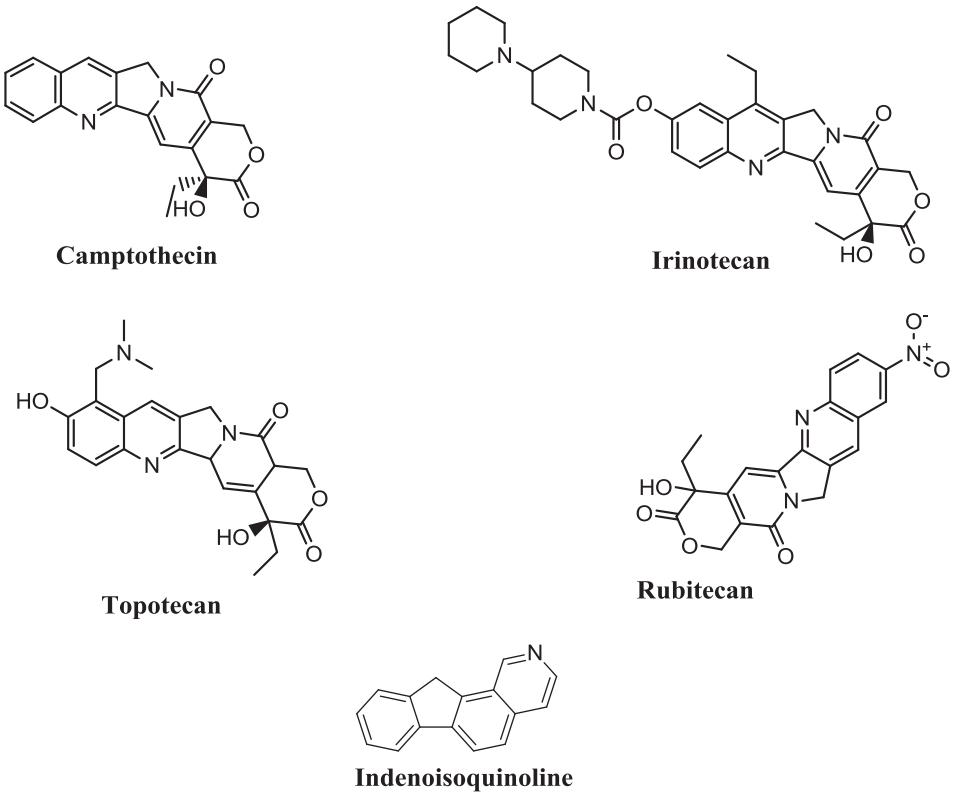

Fig. 1. Some established Topoisomerase I inhibitors as anticancer drugs.

moieties depending on their structural framework. Acridine and its analogs have fascinated the synthetic and medicinal chemists across the globe owing to their various uses [17]. It is among one of the several pharmacologically active scaffold in medicinal chemistry with biological activities like antimicrobial [18], anticancer [17,19,20], antimalarial [21], antiviral [22], anti-alzheimer [23] etc. Due to its planar structure, it can easily slid between the bases of double stranded DNA and interact with its machinery during replication, transcription and chromosome segregation [17]. Considering the promising therapeutic effects of acridine, we synthesized of new series of 9-(2-(1-phenylethylidene)hydrazinyl)acridine analogs with an objective to develop effective and safe anticancer agents against Top1(Fig. 2) [41,42].

2. Results and discussion

The title compounds (**4a–4j)** were synthesized in three steps as outlined in the synthetic protocol (Scheme 1). 2-Chlorobenzoic acid (**1**) yielded 2-(phenylamino)benzoic acid (**2**) on condensation with aniline using copper/copper oxide, anhydrous potassium carbonate in Dimethyl formamide (DMF). Compound (**2**) on cyclization with phosphorous oxychloride ($POCl_3$) afforded 9-chloroacridine (**3**) in good yield. A series of different acetophenone hydrazones were condensed with 9-chloroacridine (**3**) to yield final compounds (**4a–4j).** The purity of compounds was determined by thin layer chromatography and melting point measurement. Data from IR, ^{1}H NMR, ^{13}C NMR spectroscopy and mass spectrometry were used for the structural establishment of the synthesized compounds.

9-(2-(1-phenylethylidene)hydrazinyl)acridine derivatives **4a–4j** exhibited IR absorption for N−H at 3200–3300 cm^{-1}. The characteristic ^{1}H NMR peaks of NH proton, for compounds **4a–4j** were found around δ 10.7 ppm. In the ^{13}C NMR spectra of compounds **4a–4j**, C=N carbon peaks were observed near δ 160 ppm. Mass spectra of some of the title compounds exhibited a molecular ion peak M+ at an *m/z* equivalent to their molecular formula (see supplementary data).

2.1. In vitro antioxidant activity

2.1.1. DPPH free radical scavenging assay

The radical scavenging potential of synthesized compounds was determined by DPPH assay and compounds (**4b** and **4e)** showed remarkable antioxidant activities (Fig. 3a). These compounds showed notable DPPH radicals inhibition in a dose-dependent manner at different concentrations (5–400 μM). The free radical-scavenging action of compounds increased steadily from 5 to 100 μM and then become nearly constant. At a concentration 100 μg/ml, the radical inhibition by **4b** and **4e** were found to be 97.01 and 97.24% respectively as compared to **L-AA** which exhibited scavenging activity of 96.11%. The calculated EC_{50} values of **4b** and **4e** were 9.55 ± 0.26 μM and 9.31 ± 0.32 μM ($P < 0.05$) respectively compared to 9.65 ± 0.11 μM for L-AA (Table 1).

2.1.2. Superoxide radical scavenging assay

The outcomes depicted in Fig. 3b exhibits the superoxide radical-scavenging activity of synthesized compounds with the standard. The superoxide radical-scavenging activity of **4b** (92.14%) and **4e** (93.24%) were more significant ($P < 0.05$) compared to L-AA (89.44%) at 100 μM concentration.

2.1.3. Nitric oxide radicals

Nitric oxide free radical scavenging potential was noted to be maximum for compounds **4b** and **4e** at 400 μM concentration compared to the standard L-AA (Fig. 3c). A significant difference ($P < 0.003$) was also found in the EC_{50} values of **4b** & **4e** and the standard (Table 1).

2.1.4. Hydrogen peroxide radicals

The free radical scavenging potential of compounds was determined by hydrogen peroxide (H_2O_2) scavenging assay. Compounds **4b** and **4e** exhibited maximum scavenging effect compared to standard as shown in Fig. 3d in concentration dependent manner. The significant

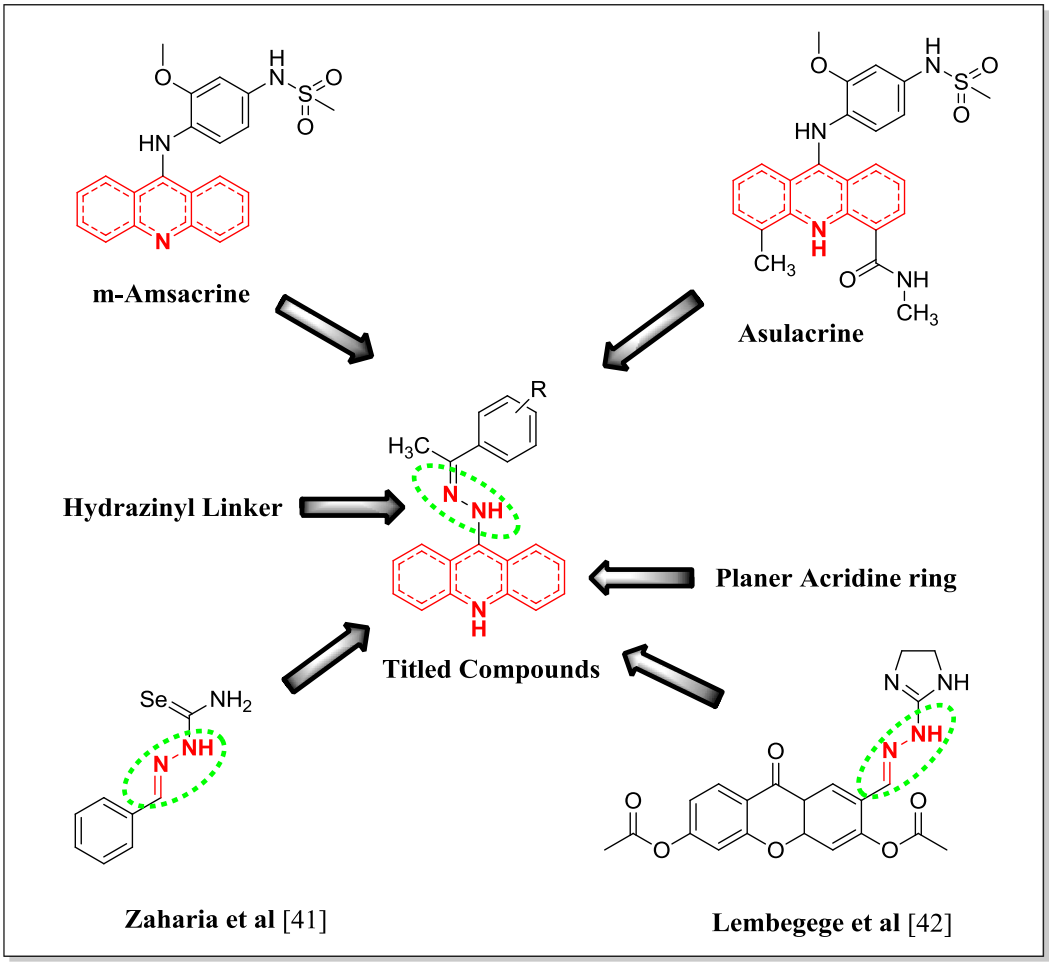

Fig. 2. Rationally designed acridine derivatives bearing hydrazinyl linker.

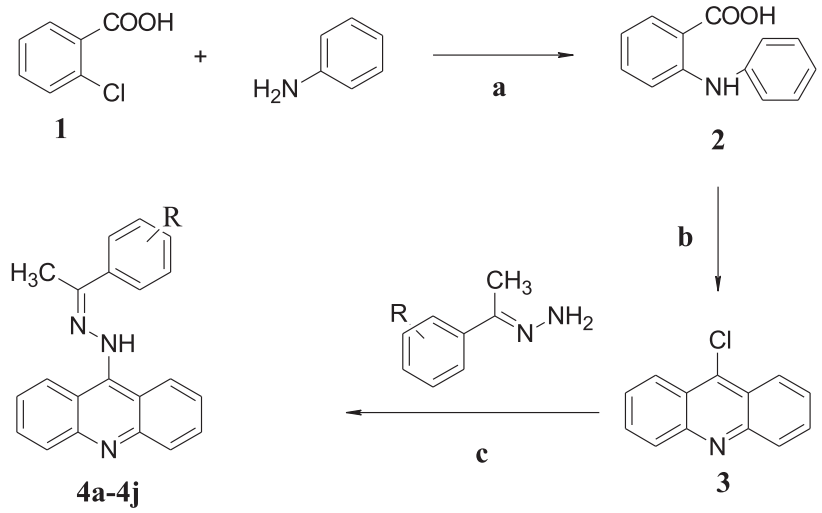

Reactions and Conditions:
a. Cu/CuO, Anhydrous K_2CO_3, DMF, reflux for 4 hrs; **b.** $POCl_3$, reflux for 3.5 hrs;
c. Abs. Ethanol, reflux 3-4 hrs.

Scheme 1. Synthetic Procedure for the synthesis of compounds **4a–4j.**

difference ($P < 0.005$) was also observed between EC_{50} values of **4b** & **4e** and the standard (Table 1).

2.1.5. Total reducing assay

The reducing power of newly synthesized compounds has been shown in Fig. 3e. In present study, free-radical scavenging potential and reducing properties of these molecules by several free-radical generating systems was performed and the quantitative estimation proved that compounds **4b** and **4e** have higher reducing power than the L-ascorbic acid. Our results suggest that antioxidant capacity of compounds **4b** and **4e** is significantly large.

2.2. In vitro anticancer activity

2.2.1. MTT assay

The in vitro cytotoxic activity of synthesized compounds was evaluated by MTT assay method MTT (3-(4,5-dimethylthiaazol-2-yl-2,5-diphenyl tetrazolium bromide) is reduced to formazan in metabolically

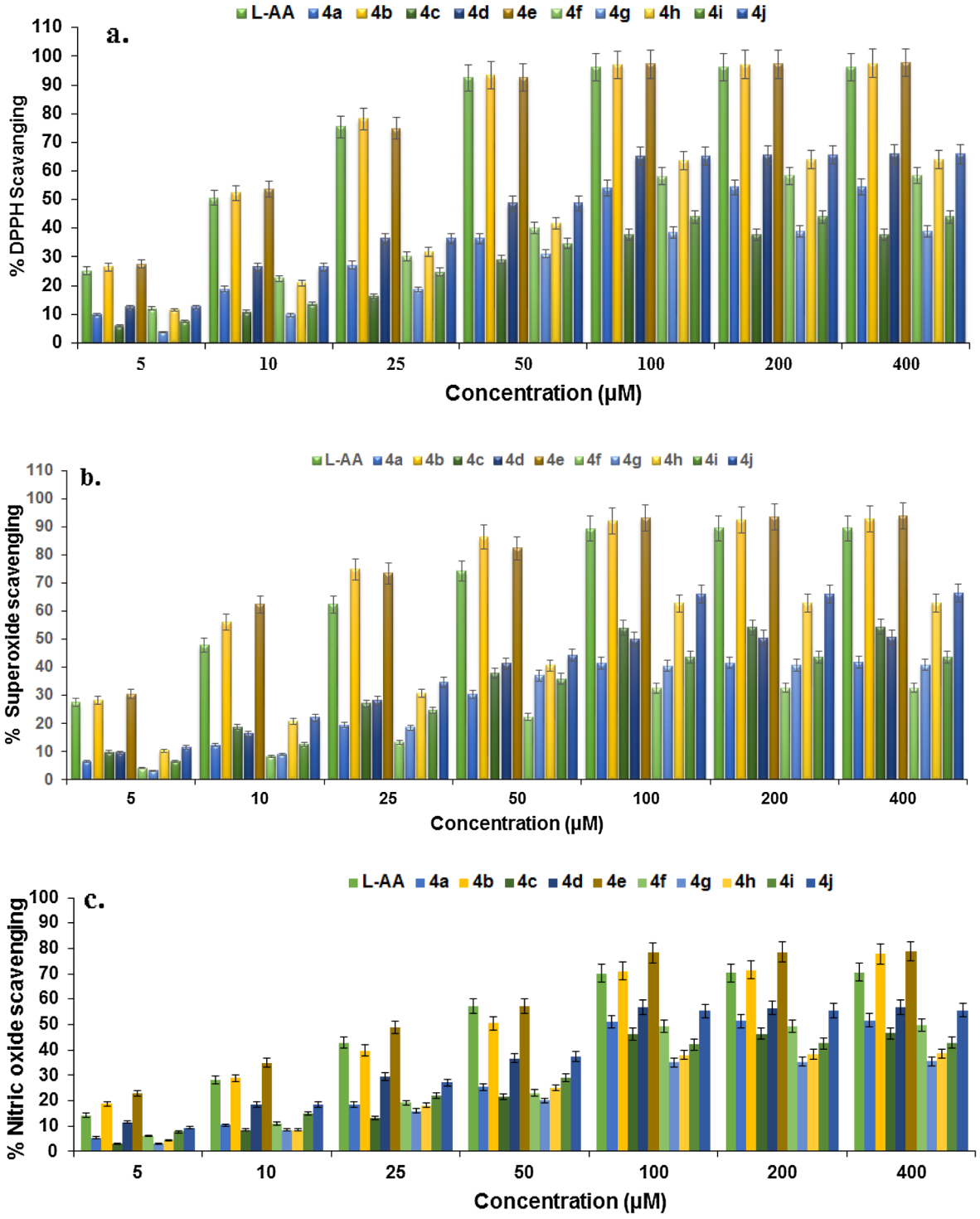

Fig. 3. Free radical-scavenging activity of compounds **4a–4j:** (a) DPPH radicals, (b) superoxide radicals, (c) hydrogen peroxide radicals and (d) nitric oxide radicals. (e) Reducing potential. L-ascorbic acid (L-AA) were considered as standard antioxidants. The values are expressed as mean ± standard deviation (n = 3) and $p < 0.05$ compared with the control.

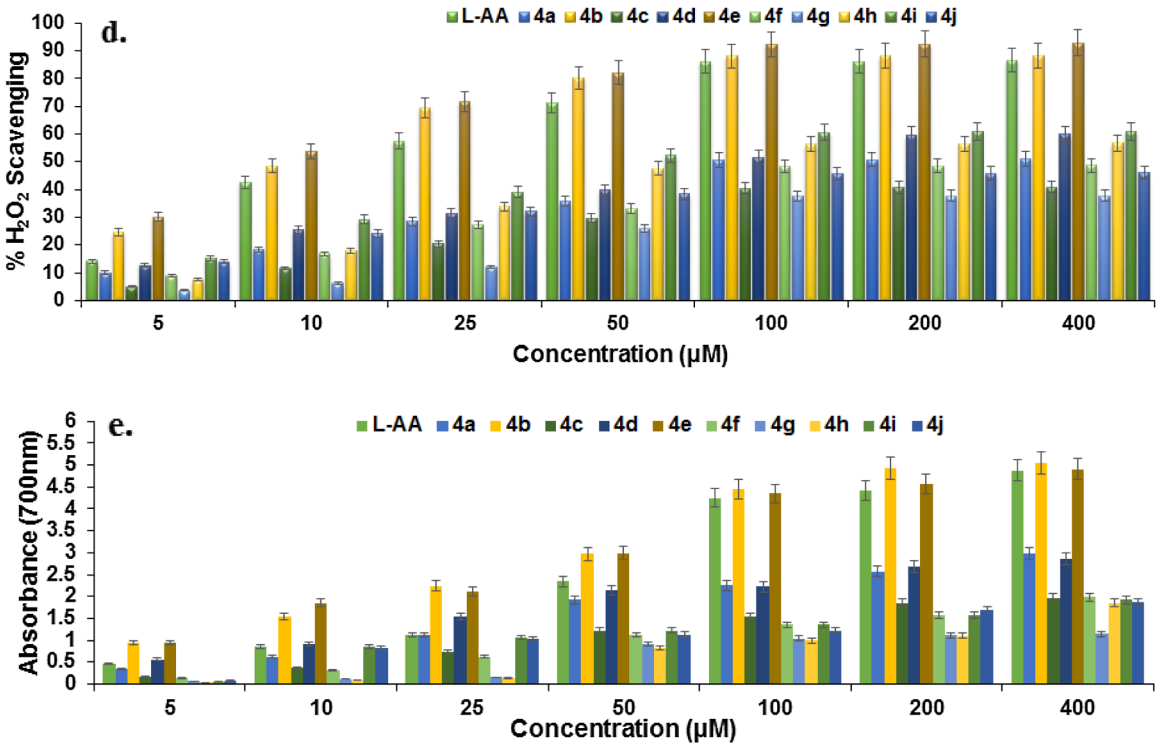

Fig. 3. (*continued*)

active cells. The MTT assay reveals that with the increase in absorbance, the viability of cells also increases and the cell inhibition decreases. The reduction in absorbance represents the cell inhibition. This is a reliable method to determine cytotoxicity of compounds. Synthesized compounds (**4a–4j**) were tested against the human embryonic kidney cells (HEK293) for cytotoxicity activity with Camptothecin as standard (Fig. 4A). IC_{50} values of compounds (**4a–4j**) against HEK293 cells were in the range 31.38–277.13 μM respectively (Table 2). The anticancer activity of compounds (**4a–4j**) against HeLa and HepG2 cell lines with increasing concentration exhibited a significant reduction in cells viability when compared to Camptothecin as standard. In case of cell proliferation assay on ovarian cancer cell line (HeLa), with increasing concentrations of compounds (**4a–4j**), varying degree of % growth inhibition was observed (Fig. 4B). The IC_{50} values of compounds were calculated and found to be in the range of 18.89–52.64 μM (Table 2). Compounds **4b** (20.97 μM), **4d** (18.89 μM) and **4e** (20.66 μM) showed the lower IC_{50} values than standard (24.00 μM), which suggests that these compounds are more active against HeLa. Cell proliferation assay against liver cancer cells (HepG2) exhibited varying degree of % growth inhibition (Fig. 4C). The IC_{50} values of compounds were calculated and found to be in the range of 18.7–108.34 μM (Table 2). Compounds **4b** (95.76 μM), **4d** (84.93 μM)

Table 1
Scavenging activity of compounds

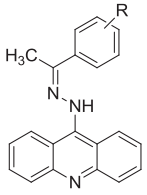

.

S No.	Compounds	R	(DPPH) EC_{50} (μM) ± S.D	Superoxide EC_{50} (μM) ± S.D	Hydrogen peroxide EC_{50} (μM) ± S.D	Nitric oxide EC_{50} (μM) ± S.D
1	**4a**	H	88.41 ± 0.41	> 400.00 ± 0.20	97.84 ± 0.36	97.71 ± 0.39
2	**4b**	4-OH	9.55 ± 0.26	8.9 ± 0.41	11.1 ± 0.29	23.39 ± 0.28
3	**4c**	4-OCH_3	> 400.00 ± 0.32	87.23 ± 0.15	> 400.00 ± 0.30	> 400.00 ± 0.31
4	**4d**	4-CH_3	53.94 ± 0.35	99.79 ± 0.17	92.88 ± 0.10	83.23 ± 0.23
5	**4e**	2-OH	9.31 ± 0.32	8.04 ± 0.40	9.24 ± 0.19	28.29 ± 0.14
6	**4f**	2-CH_3	77.57 ± 0.25	> 400.00 ± 0.16	> 400.00 ± 0.54	> 400.00 ± 0.24
7	**4g**	2-OCH_3	> 400.00 ± 0.45	> 400.00 ± 0.32	> 400.00 ± 0.76	> 400.00 ± 0.34
8	**4h**	4-Cl	68.84 ± 0.50	71.09 ± 0.49	63.25 ± 0.55	> 400.00 ± 0.41
9	**4i**	2-Cl	> 400.00 ± 0.21	> 400.00 ± 0.43	45.76 ± 0.78	> 400.00 ± 0.89
10	**4j**	3-Cl	53.95 ± 0.22	62.94 ± 0.34	> 400.00 ± 0.11	85.07 ± 0.76
11	**L-AA**		9.65 ± 0.11	12.13 ± 0.46	17.45 ± 0.19	37.34 ± 0.26

Values are expressed as mean ± standard deviation (n = 3). L-Ascorbic acid (L-AA) was used as a standard. EC_{50} value is defined as the amount of antioxidant necessary to decrease the radical concentration by 50%.

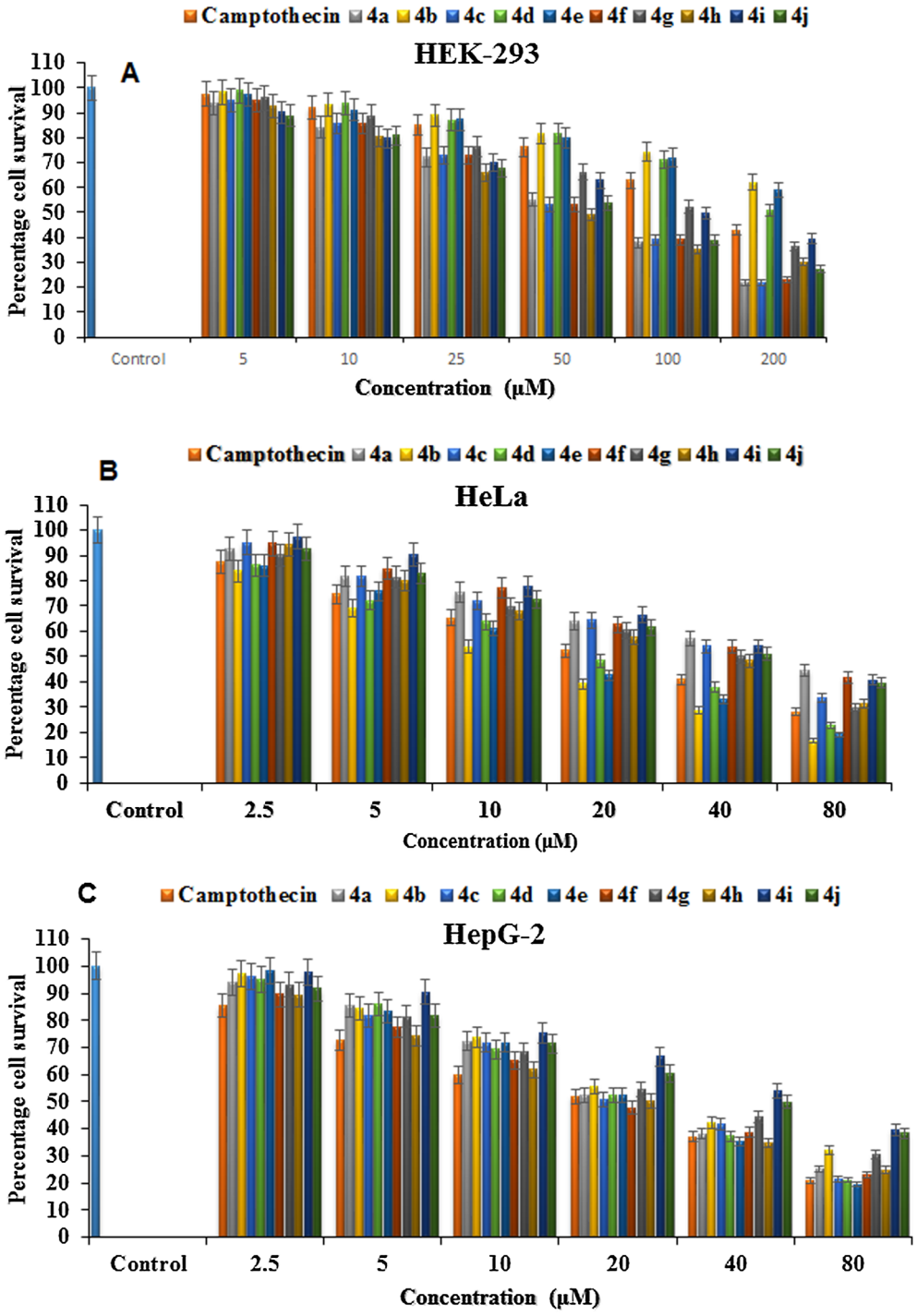

Fig. 4. Cytotoxicity assay: (A). Compounds on HEK293 cells. (B) Compounds on Hela cells and (C). Compounds on HepG-2 cells. Data represent three independent tests of experiments and results are shown as the mean ± SD. Camptothecin is used as a positive control. $p < 0.05$ compared with the control.

and **4e** (108.34 µM) showed the lowest IC_{50} values against HepG2 compared to standard (22.58 µM).

The selectivity index (SI) values for the effectiveness of selected compounds against cancerous cells were calculated. High SI value (> 3) of a compound suggests selective inhibition towards cancer cells. While the compounds with SI value < 3 is considered to be toxic for normal cells [39]. Compounds **4b**, **4d** and **4e** exhibited better selectivity against HeLa cell lines since their SI values were more than 3 compared to other compounds of the series (Table 2). The SI values of compounds **4b**, **4d** and **4e** were found to be less than 3 against HepG2 cell lines. The result suggests that compounds **4b**, **4d** and **4e** are selective and effective against HeLa cell line. Besides, the effect of the compounds **4b**, **4d** and **4e** on HeLa cells showed profound anti-proliferative activity in comparison to standard which was further complemented by cell migration assay, cell nuclear morphology assay and cell cycle analysis.

2.2.2. Structure activity relationship of 9-(2-(1-arylethylidene)hydrazinyl) acridine derivatives

On the basis of various free radical scavenging assays performed, it was inferred that compounds **4b** and **4e** exhibit excellent antioxidant potential due to presence of hydroxyl group attached to the aromatic

Table 2
IC_{50} (μM) and selectivity index (SI) values of compounds on HEK293, Hela and HepG2 cell lines (Values are expressed as mean ± standard deviation; n = 3)

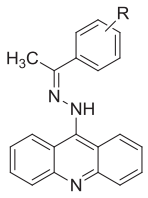

.

S.No	Compounds	R	HEK293	Hela		HepG2	
			IC_{50}(μM) ± S.D.	IC_{50}(μM) ± S.D.	SI	IC_{50}(μM) ± S.D.	SI
1	**4a**	H	50.56 ± 0.60	36.29 ± 0.57	1.39	23.43 ± 0.53	2.15
2	**4b**	4-OH	277.13 ± 0.67	20.97 ± 0.55	13.21	95.76 ± 0.65	2.89
3	**4c**	4-OCH_3	46.09 ± 0.35	34.79 ± 0.85	1.32	21.53 ± 0.54	2.14
4	**4d**	4-CH_3	206.34 ± 0.57	18.89 ± 0.61	10.92	84.93 ± 1.29	2.42
5	**4e**	2-OH	248.35 ± 0.63	20.66 ± 0.60	12.02	108.34 ± 2.23	2.29
6	**4f**	2-CH_3	46.09 ± 0.55	52.64 ± 1.50	0.87	18.7 ± 1.33	2.46
7	**4g**	2-OCH_3	104.05 ± 0.52	40.12 ± 1.56	2.59	47.06 ± 1.74	2.21
8	**4h**	4-Cl	31.38 ± 0.74	36.31 ± 1.44	0.86	20.3 ± 0.30	1.54
9	**4i**	2-Cl	91.16 ± 0.31	52.21 ± 1.50	1.74	51.5 ± 0.47	1.77
10	**4j**	3-Cl	53.45 ± 0.94	43.67 ± 1.49	1.22	39.94 ± 1.12	1.33
11	**Camptothecin**		150.79 ± 0.68	24.00 ± 2.12	6.28	22.58 ± 0.63	6.67

ring linked to acridine. Substitution of aromatic ring with methyl group results in moderate antioxidant activity while methoxy group caused poor activity. Substitution at *ortho* position results in better activity than *para* substitution. Anticancer activity of synthesized compounds performed by MTT assay against HeLa cells showed that compounds **4b, 4d** and **4e** possessed better activity than standard drug. Substitution in aromatic ring linked to acridine scaffold at *ortho* position resulted in better activity than *para* substitution. Presence of hydroxyl group at both positions resulted in more or less equal growth inhibition. Substitution with methyl group at ortho position improves the activity but at para position, there is considerable decrease in activity. All three compounds inhibited of Top1 enzyme during inhibition assay. Anticancer potential of all the three compounds has been further supported by molecular docking.

2.2.3. Cell nuclear morphology assay

Necrotic and apoptotic cells were observed through fluorescence microscopy technique (Nikon Eclipse, Inc., Japan) on the basis of cell membrane integrity and general cell morphology. Initially, fluorescence microscopic evaluation showed untreated HeLa cells tainted with a uniform blue fluorescence and intact shape. 48 h post treatment with compounds **4b**, **4d** and **4e** at IC_{50} concentrations, the cells were observed for morphological alterations as shown in Fig. 5A.

Mean and the standard deviations were also calculated based on numbers of apoptotic cells. An increase was observed in number of apoptotic cells at IC_{50} concentration of **4b**, **4d** and **4e** (Fig. 5B). Percentage of apoptotic cells was determined for being statistically significant from the **4b**, **4d** and **4e** treated HeLa cancer cells. Only a small fraction of apoptotic cells were found in the control cells.

2.2.4. Cell migration assay

The wound-healing study to determine cell migration demonstrated considerable decrease in cell migration on treatment with compounds **4b**, **4d** and **4e** at IC_{50} concentrations in HeLa cells. Photomicrographs of HeLa cells post treatment with **4b**, **4d** and **4e** is shown in Fig. 5a. The wound closure rate images were taken after 48 h treatment. Scale bars were added with the help of Image J, as depicted in Fig. 5b. As shown in Fig. 5a, wound area significantly increased on treatment with compounds **4b**, **4d** and **4e** after 48 h. However, in control cells a reduction in area was observed. Besides, it was observed that **4b**, **4d** and **4e** exhibited better reduction in cell migration compared to control (Fig. 5a & Fig. 5b).

2.2.5. Effect on cell cycle regulation

The cell cycle analysis in HeLa cells on treatment with compounds **4b**, **4d** and **4e** was studied by flow cytometry using propidium iodide staining technique. The percentage of apoptotic cells as well as cell cycle stage 48 h post treatment with compounds is shown in Fig. 5I & II. Treatment with compounds **4b**, **4d** and **4e** at IC_{50} concentrations in HeLa cells induce 12.4%, 2.4%, and 11.7% of apoptosis, respectively compared against the untreated control (1.4%) as presented in Fig. 5I.

Treatment of HeLa cells with compounds **4b**, **4d** and **4e** at IC_{50} concentration caused an increase in the percentage of cells in the S phase against control. Compound **4b** also resulted in rise of cells in G0/G1 phase against control. The percentage of cells got reduced in G2/M phase in comparison to control cells. The flow cytometry analysis suggested that the effect of compounds **4b**, **4d** and **4e** on the accumulation of cells in the S phases subsequently resulted in cell cycle arrest (Fig. 5I & II).

2.3. Topoisomerase 1(Top1) inhibition assay

Top1 is a key cellular enzyme that cuts DNA and makes it to wind and unwind, thereby plays an important role in transcription, replication and chromosome structure. The strategy to inhibit Top1 enzyme leads to death of cancer cells, thereby acts as target in human cancer chemotherapy. In order to study the possible mechanism of cytotoxic potential exhibited by synthesized compounds **4b, 4d** and **4e** were subjected to DNA relaxation study. The supercoiled plasmid PBR322 was incubated with human Top1 in the presence of the test compounds at 2 μM concentration each. As shown in Fig. 5III, compounds **4b, 4d** and **4e** showed Top1 inhibitory activity based on position of supercoiled DNA. Based on the study, it is suggested that compounds **4b, 4d** and **4e** exhibit anticancer activity through Top1 inhibition.

2.4. Molecular docking studies

Molecular docking was performed in order to establish the binding ability of the new synthesized compounds with Top1. The docking scores of all compounds are presented in Table 3. All the compounds

were found to exhibit good interaction with the target protein.

Among all the titled compounds tested for Top1 inhibition, **4b** was found to be most potent and have highest docking score (−6.8 Kcal/mol) as compared to Camptothecin (Table 3). Compound **4b** demonstrated two hydrogen bonds-one each with DNA residue (DA113; 2.3 Å) and Top1 residue (GLU356; 3.4 Å) (Fig. 6A(II)). The compound **4b** also assumes favorable orientation within the Top1-DNA complex binding site by interacting with other residues (DC112, ASN352,

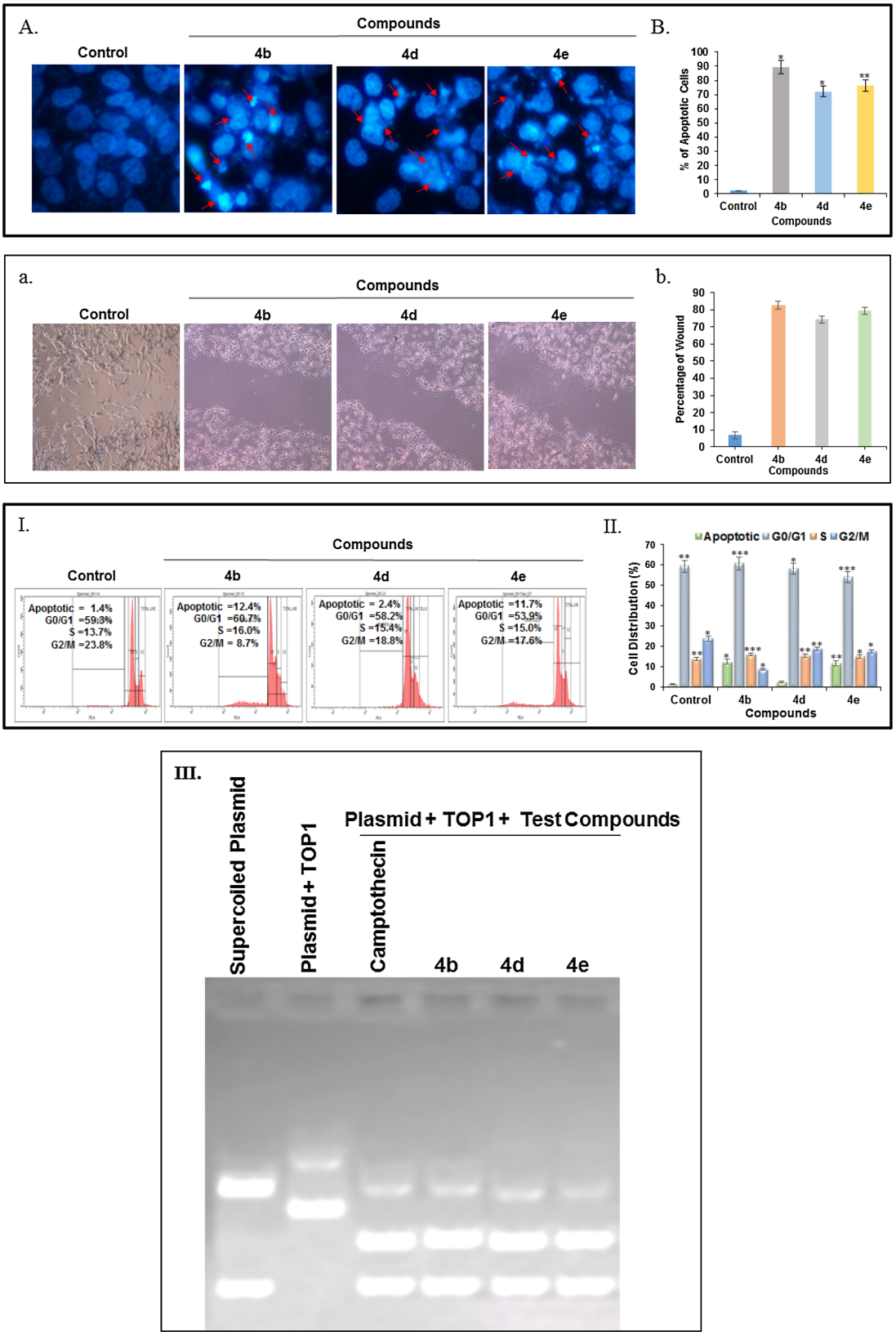

(caption on next page)

Fig. 5. Effect of compounds on HeLa cells: *Cell nuclear morphology:* (A) without treatment compound (Control), treated with compounds **4b, 4d** and **4e**. (B) Percentage of apoptotic cells against their IC_{50} concentrations of compounds **4b, 4d** and **4e**. *Cell migration:* (a) Width of wound increases effectively after the treatment of compounds **4b, 4d** and **4e** in HeLa cell lines as compared without treatment compound (Control). (b) The percentage of wound against their IC_{50} concentrations of compounds **4b, 4d** and **4e** as compared without treatment of compound (Control). *Cell cycle regulation:* (I) Cell cycle phase distribution with treatment of compounds **4b, 4d** and **4e** as compared without treatment of compound (Control). Compounds **4b** arrests HeLa cell cycle in G0/G1 and S phase while **4d** and **4e** arrests HeLa cell cycle in S phase as determined by flow cytometry. (II) Bar graph indicating cell distribution percentage against IC_{50} concentrations of compounds **4b, 4d** and **4e** as compared without treatment of compound (Control). (III) Top1 inhibition assay of compounds **4b, 4d** and **4e** depicting the relaxation of supercoiled pBR322 plasmid DNA as compared to Camptothecin. Data represent three independent tests of experiments and results are shown as the mean ± SD.$p < 0.05$ compared with the control. Representative images (40X magnification) by fluorescence microscope.

ARG364, LYS374, TRP416, GLU418, LYS425, TYR426 and ILE427) as against Camptothecin shown in Table 3 and Fig. 6A(I). Compound **4d** showed no hydrogen bonding with Top1-DNA complex, but exhibited other kinds of interactions with various residues of Top1-DNA complex (DC112, DA113, ASN352, GLU356, PHY361, ARG364, LYS374, TRP416, GLU418, LYS425, TYR426 and ILE427) presented in Fig. 6B(i) & 6B(ii). Compound **4e** interacted through hydrogen bonds-one each with DNA residue (DA112; 2.9 Å) and Top1 residue (ARG364; 2.0 Å) as compared to Camptothecin shown in Table 3. The compound **4e** also interacts with the Top1-DNA complex binding site by interacting with other residues (DA113, ASN352, GLU356, PHY361, ARG364, LYS374, TRP416, GLU418, LYS425, TYR426 and ILE427) shown in Fig. 6C(a). In the Table 3, Camptothecin- an inhibitor of Top1 interacted through one hydrogen bond with Top1-DNA complex (ARG364; 2.4 Å). It interacts with the Top1-DNA complex binding site by interacting with other residues (DC112, DA113, ASN352, GLU356, LYS374, TRP416, GLU418 and LYS425).

Molecular docking study of compounds suggested that several Van der Waals, covalent, carbon hydrogen, Pi alkyl and electrostatic interactions are the key force for bonding of compounds **4b, 4d** and **4e** together with the Top1. Furthermore, compounds **4b, 4d** and **4e** interact to the Top1 supported that the antiproliferative activity of synthesized compounds is caused due to inhibition of Top1 [40,41]. Compounds **4b, 4d** and **4e** bind to Top1 with excellent docking score and it may be considered as an appreciable inhibitor of the Top1.

Schematic model representing inhibition of Top1 by compounds **4b, 4d** and **4e** is shown in Fig. 7. Compounds **4b, 4d** and **4e** bind to Top1 that can block the DNA replication and ultimately arrest the cell cycle in S phase and subsequent induction of apoptosis reduce the malignant alteration of cells.

3. Conclusion

It is evident from the results that the presence of hydroxyl group attached to the aromatic ring linked to acridine in compounds **4b** and **4e** might be responsible for its antioxidant behavior. Cellular experimental results revealed that compounds **4b, 4d** and **4e** inhibited cell growth and cell migration predominately in cervical cancer cell. Death of cancer cells by compounds **4b, 4d** and **4e** especially followed apoptosis. A possible S phase arrest might be due to the inhibition of Top1 activity and triggered apoptosis. The mechanism of action of the compounds **4b, 4d** and **4e** in cervical cancer cell could possibly be target Top1 and prevents it DNA replication. In silico experimental results unveiled that the van der Waals, covalent, carbon hydrogen, Pi alkyl and electrostatic interactions are the key force responsible for better interaction of compounds present in **4b, 4d** and **4e** with the Top1. Moreover, our results suggested that compounds **4b, 4d** and **4e** decreases the cell growth of cervical cancer cell lines by inhibition of Top1 and could be effectively used in the cancer chemoprevention and chemotherapy.

4. Material and methods

4.1. General information

Melting points of synthesized compounds were determined using open capillary method and are uncorrected. Progress of the reactions was monitored using self prepared TLC plates (silica gel 'G' as stationary phase) and TEF (Toluene: Ethyl acetate: Formic acid; 5:4:1) as mobile phase. The spots were visualized and marked by exposure to iodine vapors as well as under UV-light. Shimadzu Infra Red Spectrometer (FTIR-8400S) was used to record IR spectra by KBr pellet method. ^{1}H NMR and ^{13}C NMR spectra were recorded on Bruker – 300/400 MHz NMR spectroscope using DMSO-d_6/$CDCl_3$ as solvent media. Chemical shift values has been reported in parts per million (ppm) using TMS (tetramethylsilane) as internal reference. D_2O exchange method was used to establish OH and NH protons. LCMS/MS (Perkin-Elmer and LABINDIA, Applied Biosystem) model no. API 3000 was employed to record mass and presented as *m/z*. For elemental analyses, Perkin-Elmer 240 analyzer was used and found for each element analyzed (C, H and N) in the range of ± 0.4%.

MTT (3-[4,5-dimethylthiazol-2-yl]-2,5-diphenyl tetrazolium bromide), 1,1-Diphenyl-2-picrylhydrazyl (DPPH), 2,4,6-tri (2-pyridyl)-s-triazine (TPTZ) and Ascorbic acid were obtained from Sigma Aldrich (Steinheim, Germany) and DMSO was purchased from Merck. Cell lines HeLa, HepG2 and HEK293 were procured from National Centre for Cell Sciences (NCCS), Pune, India. Dulbecco's Modified Eagle's Media (DMEM) and Fetal bovine serum were taken from Gibco-life technologies.

Table 3
Parameters obtained from molecular docking studies of Topoisomerase 1 (PDB ID: 1T8I) with compounds.

Compound	GScore (Kcal/mol)	No. of Hydrogen bonds	Hydrogen bond forming residues	Distance (Å)	Other interacting residues
4b	−6.8	2	DA113 GLU356	2.3 3.4	DC112, DA113, ASN352, ARG364, LYS374, TRP416, GLU418, LYS425, TYR426, ILE427
4d	−6.0	–	–	–	DC112, DA113, ASN352, GLU356, PHY361, ARG364, LYS374, TRP416, GLU418, LYS425, TYR426, ILE427
4e	−5.2	2	DC112, ARG364	2.9 2.0	DA113, ASN352, GLU356, PHY361, LYS374, TRP416, GLU418, LYS425, TYR426, ILE427
Known Inhibitors					
Camptothecin	−4.4	1	ARG364	2.4	DC112, DA113, ASN352, GLU356, LYS374, TRP416, GLU418, LYS425
m-Amsacrine	−3.6	3	GLU256, LYS 425. TYR 426	2.5 2.2 2.0	DC112, DA113, DA114, DG115, ALA351, ASN352, LYS354, ILE 355, ILE424, ILE427, MET428, LEU429, LYS436

Each of the newly synthesized test compounds **4a** to **4j** and standard were dissolved in 0.1% dimethyl sulfoxide (DMSO) and diluted to final concentrations of 5 to 80 μM each.

4.2. Synthesis of 9-(2-(1-phenylethylidene)hydrazinyl)acridine analogs

4.2.1. Synthesis of 2-(phenylamino)benzoic acid (2)

A mixture of 2-chlorobenzoic acid (**1**) (100 mmol) and aniline (110 mmol) in sufficient quantity of DMF containing catalytic amount of copper oxide (3.2 g) and potassium carbonate (27.6 g) was refluxed for 4 hrs. TLC was used at regular intervals to monitor the progress and completion of reactions. Once the reaction was complete, the reaction mixture was cooled down to room temperature, poured in to ice-cold water with stirring, filtered and neutralized with conc. HCl. The precipitate thus obtained was filtered, dried and recrystallized from a mixture of ethanol-water (Yield 74%) [24].

4.2.2. Synthesis of 9-chloroacridine (3)

10 g of 2-(phenylamino)benzoic acid (**2**) was dissolved in 16 ml of freshly distilled phosphorous oxychloride and warmed on a water bath up to 80 °C for 15 min. and then refluxed for 3.5 hrs on oil bath. The progress of reaction was monitored constantly using TLC until completion. The reaction mixture was then allowed to cool down at room temperature. Excess of Phosphorous oxychloride was removed by distillation under reduced pressure. To this, a mixture of ice, ammonia and chloroform was added with vigorous stirring. The chloroform layer was separated and the aqueous layer was further extracted with chloroform. The chloroform extracts were combined and dried using rotary evaporator to get 9-chloroacridine as greenish residue. It was obtained as pure crystals using hexane (Yield 67%) [25].

4.2.3. Synthesis of 9-(2-(1-phenylethylidene)hydrazinyl)acridine and its analogs (4a-4l)

To the ethanolic solution of 9-chloroacridine (2 mmol) and different acetophenone hydrazones (2 mmol) [26], 2–3 drops of conc. HCl were added and the reaction mixture was refluxed for 3–4 hrs. TLC was taken at regular time intervals to monitor the reaction. Once the reaction was complete, the reaction mixture was allowed cooled to room temperature and filtered to obtain the crystals of final product.

4.2.3.1. 9-(2-(1-phenylethylidene)hydrazinyl)acridine (4a). Yield 72%, m.p. 212–214 °C, IR (KBr; cm^{-1}): 3269 (N—H str.), 3117 (Ar.C—H str.), 2878 (Ali. C—H str.); ^{1}H NMR (400 MHz, DMSO-d_6, δ ppm): 2.46 (3H, s, CH_3), 6.92–6.96 (2H, t, Ar.H), 7.09–7.12 (2H, m, Ar.H),

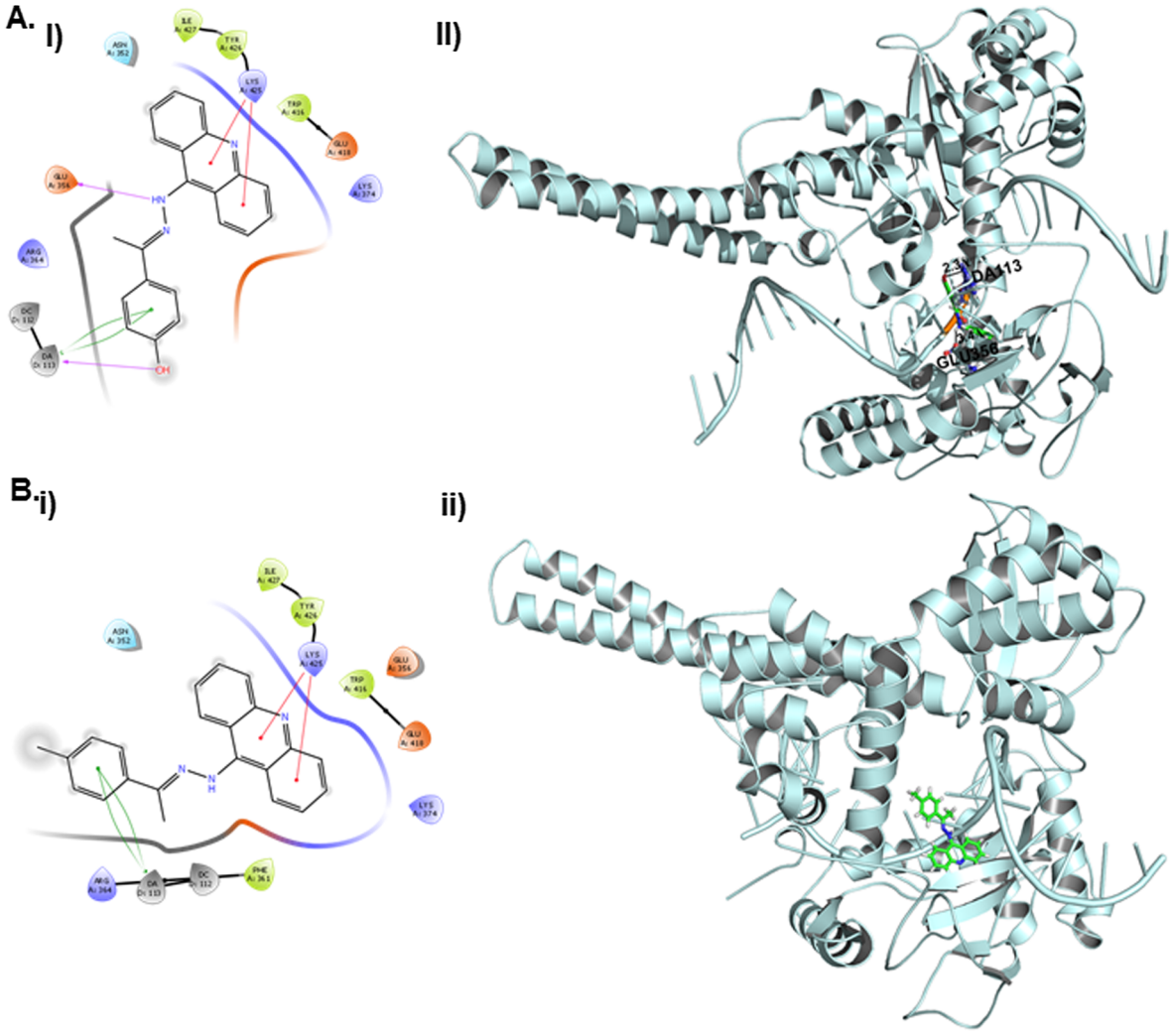

Fig. 6. Molecular docking of compounds with Top1 (PDB ID: 1T8I): (A) (I) 2D schematic diagram showing interactions of compound **4b**. (II) Cartoon view of Top1 protein with compound **4b**. (B) (i) 2D schematic diagram showing interactions of compound **4d**. (ii) Cartoon view of Top1 protein with compound **4d**. **C**) (a) 2D schematic diagram showing interactions of compound **4e**. (b) Cartoon view of Top1 protein with compound **4e**. **D)** (I) 2D schematic diagram showing interactions of m-Amsacrine. (II) Cartoon view of Top1 protein with m-Amsacrine. Residues involved in hydrogen bonding, van der Waals interactions, carbon hydrogen and Pi-alkyl are represented in different color indicated in inset.

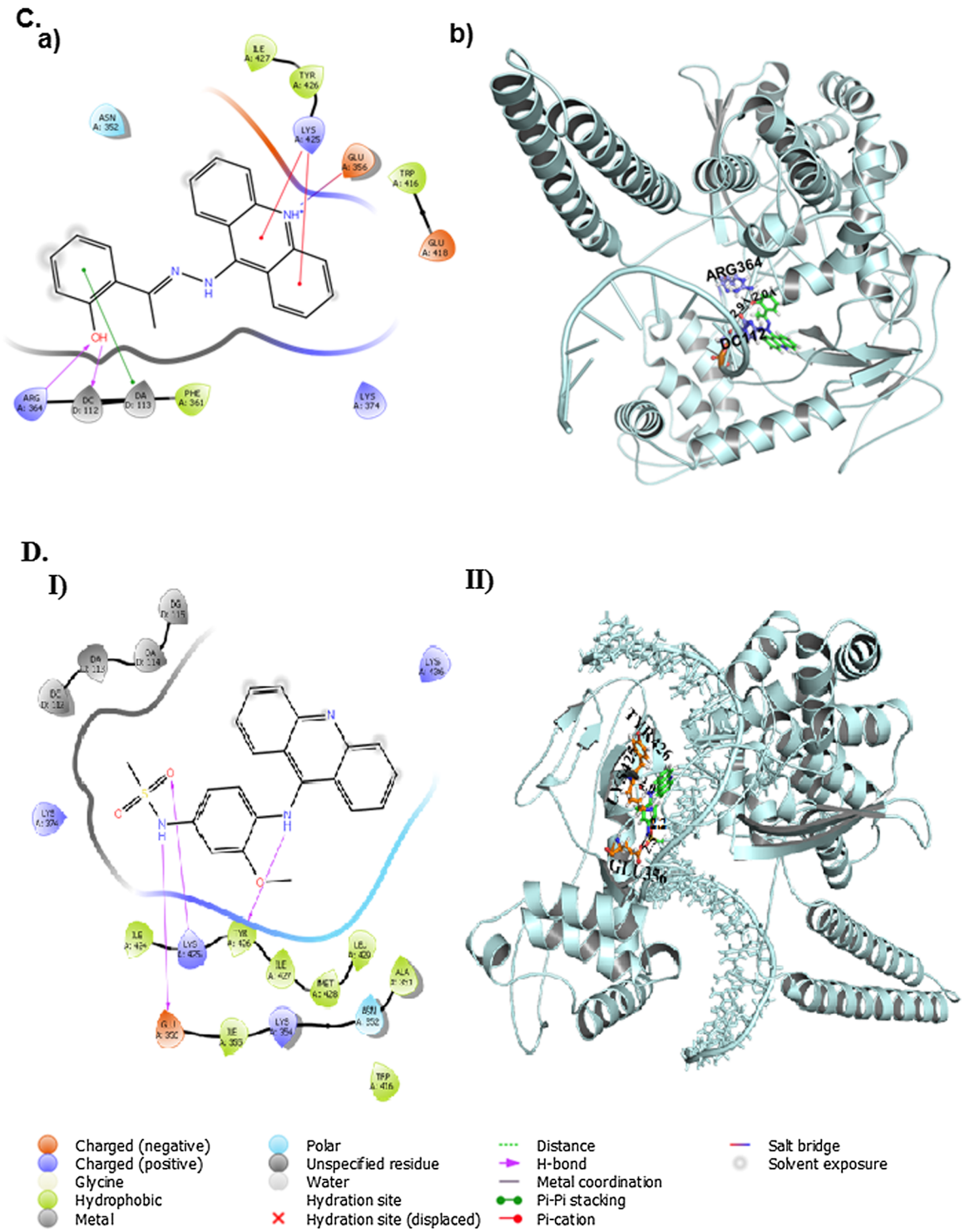

Fig. 6. (*continued*)

7.22–7.26 (3H, m, Ar.H), 7.45–7.50 (2H, t, Ar.H), 7.96–7.98 (2H, d, Ar.H), 8.29–8.39 (1H, q, Ar,H), 8.57–8.59 (1H, d, Ar,H), 10.71 (1H, s, NH); ^{13}C NMR (100 MHz, $CDCl_3$, ppm): 15.0, 76.6, 77.4, 126.6, 128.4, 129.6, 138.5, 157.7; LC-MS (*m/z*): 312 [M + 1]; Elem. Anal. Calc. for $C_{21}H_{17}N_3$: C, 81.00; H, 5.50; N, 13.49. Found: C, 81.03; H, 5.48; N, 13.47.

4.2.3.2. 4-(1-(2-(acridin-9-yl)hydrazono)ethyl)phenol (4b). Yield 72%, m.p. 220–222 °C, IR (KBr; cm^{-1}): 3249 (N—H str.), 3107 (Ar.C—H str.), 2888 (Ali. C—H str.); ^{1}H NMR (300 MHz, DMSO-d_6, δ ppm): 2.51 (3H, s, CH_3), 5.35 (1H, s, —OH), 7.21–7.26 (2H, t, Ar.H), 7.50–7.61 (2H, m, Ar.H), 7.69–7.75 (2H, m, Ar.H), 7.85–7.89 (2H, t, Ar.H), 8.14–8.16 (2H, d, Ar.H), 8.22–8.24 (1H, d, Ar,H), 8.42–8.47 (1H, d, Ar,H), 11.76 (1H, s, NH); ^{13}C NMR (75 MHz, $CDCl_3$, ppm): 15.0, 76.6, 77.4, 126.6, 128.4, 129.6, 138.5, 157.7, 162.10; LC-MS (*m/z*): 328 [M + 1]; Elem. Anal. Calc. for $C_{21}H_{17}N_3O$: C, 77.04; H, 5.23; N, 12.84. Found: C, 77.54; H, 5.18; N, 12.77.

4.2.3.3. 9-(2-(1-(4-methoxyphenyl)ethylidene)hydrazinyl)acridine (4c). Yield 62%, m.p. 198–200 °C, IR (KBr; cm^{-1}): 3263 (N—H str.),

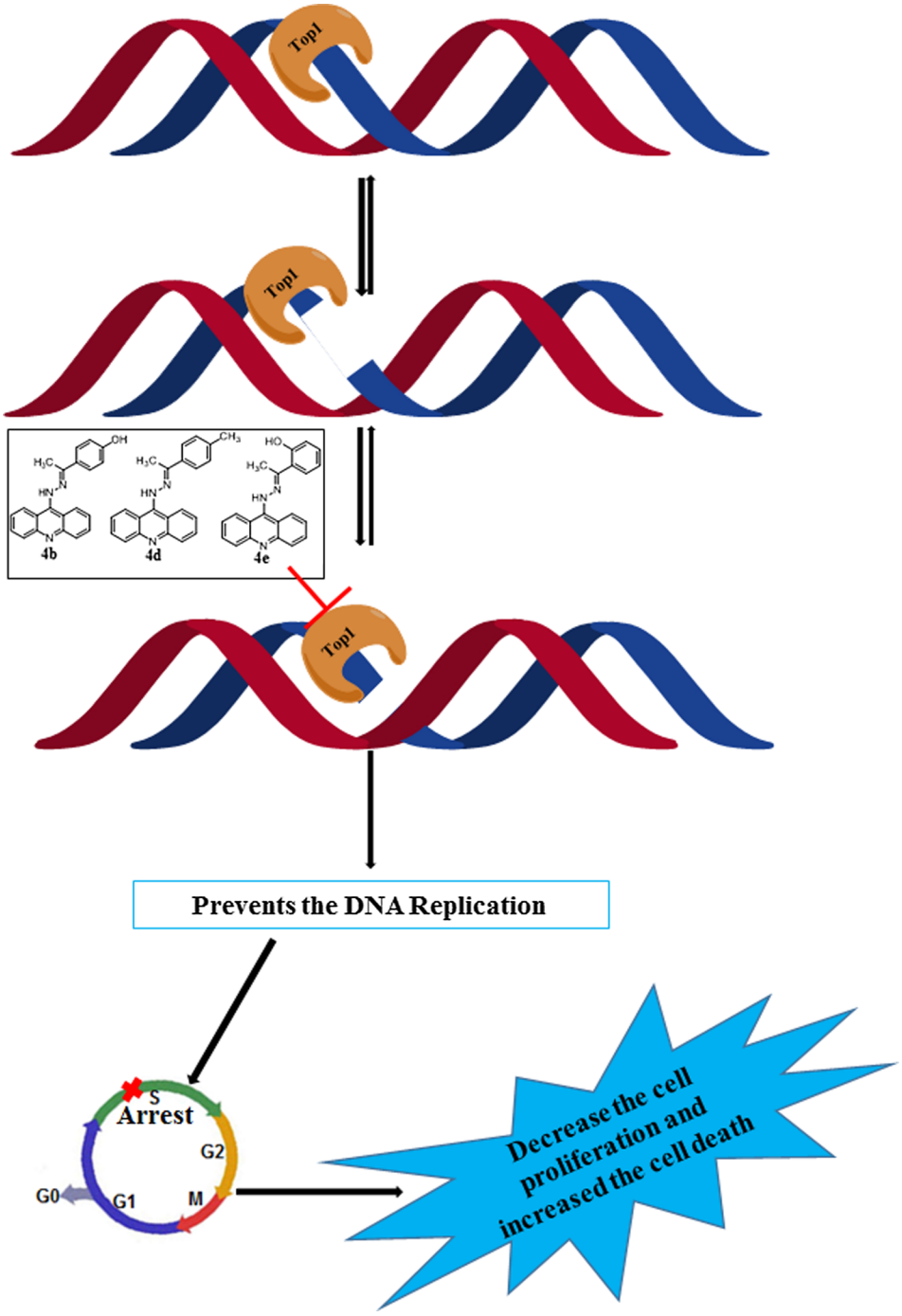

Fig. 7. Proposed schematic model for the inhibition of Top1 by compounds **4b, 4d** and **4e**.

3121 (Ar.C—H str.), 2858 (Ali. C—H str.); ^{1}H NMR (300 MHz, DMSO-d_6, δ ppm): 2.50 (3H, s, CH_3), 3.79 (3H, s, OCH_3), 7.22–7.27 (2H, t, Ar.H), 7.50–7.61 (2H, m, Ar.H), 7.69–7.75 (2H, m, Ar.H), 7.84–7.89 (2H, t, Ar.H), 8.14–8.16 (2H, d, Ar.H), 8.22–8.24 (1H, d, Ar,H), 8.42–8.45 (1H, d, Ar,H), 11.96 (1H, s, NH); LC-MS (*m/z*): 342 [M + 1]; Elem. Anal. Calc. for $C_{22}H_{19}N_3O$: C, 77.40; H, 5.61; N, 12.31. Found: C, 79.03; H, 5.64; N, 12.40.

4.2.3.4. 9-(2-(1-(p-tolyl)ethylidene)hydrazinyl)acridine (4d). Yield 76%, m.p. 206–208 °C, IR (KBr; cm^{-1}): 3236 (N—H str.), 3100 (Ar.C—H str.), 2890 (Ali. C—H str.); ^{1}H NMR (300 MHz, DMSO-d_6, δ ppm): 2.30 (3H, s, CH_3), 2.95 (3H, s, CH_3), 7.23–7.25 (2H, t, Ar.H), 7.50–7.61 (2H, m, Ar.H), 7.70–7.74 (2H, m, Ar.H), 7.83–7.89 (2H, m, Ar.H), 8.14–8.17 (2H, t, Ar.H), 8.23–8.25 (1H, d, Ar.H), 8.40–8.43 (1H, d, Ar,H), 11.74 (1H, s, NH); LC-MS (*m/z*): 326 [M + 1]; Elem. Anal. Calc. for $C_{22}H_{19}N_3$: C, 81.20; H, 5.89; N, 12.91. Found: C, 81.03; H, 5.78; N, 13.17.

4.2.3.5. 2-(1-(2-(acridin-9-yl)hydrazono)ethyl)phenol (4e). Yield 69%, m.p. 202–204 °C, IR (KBr; cm^{-1}): 3252 (N—H str.), 3123 (Ar.C—H str.), 2866 (Ali. C—H str.); ^{1}H NMR (300 MHz, DMSO-d_6, δ ppm): 2.40 (3H, s, CH_3), 5.34 (1H, s, OH), 7.21–7.26 (2H, t, Ar.H), 7.50–760 (2H, m, Ar.H), 7.70–7.76 (2H, d, Ar.H), 7.84–7.89 (2H, t, Ar.H), 8.14–8.17 (2H, d, Ar.H), 8.22–8.25 (1H, d, Ar,H), 8.42–8.47 (1H, d, Ar,H), 11.76 (1H, s, NH); LC-MS (*m/z*): 328 [M + 1]; Elem. Anal. Calc. for $C_{21}H_{17}N_3O$: C, 77.04; H, 5.23; N, 12.84. Found: C, 76.94; H, 5.21; N, 12.90.

4.2.3.6. 9-(2-(1-(o-tolyl)ethylidene)hydrazinyl)acridine (4f). Yield 72%, m.p. 192–194 °C, IR (KBr; cm^{-1}): 3252 (N—H str.), 3127 (Ar.C—H str.), 2898 (Ali. C—H str.); ^{1}H NMR (300 MHz, DMSO-d_6, δ ppm): 2.40 (3H, s, CH_3), 2.87(3H, s, CH_3), 7.23–7.28 (2H, t, Ar.H), 7.52–7.62 (2H, m, Ar.H), 7.70–7.76 (2H, m, Ar.H), 7.83–7.89 (2H, t, Ar.H), 8.13–8.15 (2H, d, Ar.H), 8.24–8.27 (1H, d, Ar,H), 8.40–8.43 (1H, d, Ar,H), 11.74 (1H, s, NH); LC-MS (*m/z*): 326 [M + 1]; Elem. Anal. Calc. for $C_{22}H_{19}N_3$: C, 81.20; H, 5.89; N, 12.91. Found: C, 81.33; H, 5.93; N, 13.08.

4.2.3.7. 9-(2-(1-(2-methoxyphenyl)ethylidene)hydrazinyl)acridine (4 g). Yield 78%, m.p. 188–190 °C, IR (KBr; cm^{-1}): 3268 (N—H str.), 3110 (Ar.C—H str.), 2882 (Ali. C—H str.); ^{1}H NMR (300 MHz, DMSO-d_6, δ ppm): 2.48 (3H, s, CH_3), 3.78 (3H, s, OCH_3), 7.12–7.17 (2H, t, Ar.H), 7.50–7.62 (2H, m, Ar.H), 7.69–7.74 (2H, m, Ar.H), 7.84–7.89 (2H, t, Ar.H), 8.14–8.17 (2H, d, Ar.H), 8.22–8.25 (1H, d, Ar,H), 8.42–8.45 (1H, d, Ar,H), 11.92 (1H, s, NH); LC-MS (*m/z*): 342 [M + 1]; Elem. Anal. Calc. for $C_{22}H_{19}N_3O$: C, 77.40; H, 5.61; N, 12.31. Found: C, 78.41; H, 5.59; N, 12.28.

4.2.3.8. 9-(2-(1-(4-fluorophenyl)ethylidene)hydrazinyl)acridine (4 h). Yield 62%, m.p. 210–212 °C, IR (KBr; cm^{-1}): 3270 (N—H str.), 3120 (Ar.C—H str.), 2871 (Ali. C—H str.); ^{1}H NMR (300 MHz, DMSO-d_6, δ ppm): 2.51 (3H, s, CH_3), 7.22–7.27 (2H, t, Ar.H), 7.48–7.60 (2H, m, Ar.H), 7.68–7.74 (2H, m, Ar.H), 7.84–7.89 (2H, t, Ar.H), 8.14–8.17 (2H, d, Ar.H), 8.23–8.26 (1H, d, Ar,H), 8.42–8.45 (1H, d, Ar,H), 11.86 (1H, s, NH); Elem. Anal. Calc. for $C_{21}H_{16}FClN_3$: C, 76.58; H, 4.90; N, 12.76. Found: C, 77.02; H, 4.88; N, 12.72.

4.2.3.9. 9-(2-(1-(2-chlorophenyl)ethylidene)hydrazinyl)acridine (4i). Yield 77%, m.p. 204–206 °C, IR (KBr; cm^{-1}): 3260 (N—H str.), 3110 (Ar.C—H str.), 2880 (Ali. C—H str.); ^{1}H NMR (300 MHz, DMSO-d_6, δ ppm): 2.52 (3H, s, CH_3), 7.20–7.26 (2H, t, Ar.H), 7.48–7.59 (2H, m, Ar.H), 7.69–7.75 (2H, m, Ar.H), 7.82–7.87 (2H, t, Ar.H), 8.16–8.19 (2H, d, Ar.H), 8.24–8.27 (1H, d, Ar,H), 8.44–8.47 (1H, d, Ar,H), 11.71 (1H, s, NH); Elem. Anal. Calc. for $C_{21}H_{16}ClN_3$: C, 72.93; H, 4.66; N, 12.15. Found: C, 73.02; H, 4.68; N, 12.12.

4.2.3.10. 9-(2-(1-(3-chlorophenyl)ethylidene)hydrazinyl)acridine (4j). Yield 63%, m.p. 194–196 °C, IR (KBr; cm^{-1}): 3274 (N—H str.), 3137 (Ar.C—H str.), 2865 (Ali. C—H str.); ^{1}H NMR (300 MHz, DMSO-d_6, δ ppm): 2.53 (3H, s, CH_3), 7.21–7.26 (2H, t, Ar.H), 7.49–7.61 (2H, m, Ar.H), 7.68–7.75 (2H, m, Ar.H), 7.82–7.86 (2H, t, Ar.H), 8.15–8.18 (2H, d, Ar.H), 8.23–8.26 (1H, d, Ar,H), 8.42–8.44 (1H, d, Ar,H), 11.74 (1H, s, NH); Elem. Anal. Calc. for $C_{21}H_{16}ClN_3$: C, 72.93; H, 4.66; N, 12.15. Found: C, 73.02; H, 4.68; N, 12.12.

4.3. Determination of in vitro antioxidant activity

The antioxidant potential of *synthetic derivatives of 9-chloroacridine* was determined by different free radical-scavenging assays. Experiments were performed in triplicate taking L-ascorbic acid as standard.

DPPH radical-scavenging assay was carried out as per the standard procedure previously reported by Miliauskas [27]. Superoxide radical-scavenging potential was determined by the process developed by Liu with minor changes [28]. Hydrogen peroxide (H_2O_2) assay was done to measure the scavenging capacity using the method reported earlier by Ruch with slight modification [29]. Griess assay method was employed for Nitric oxide free radical-scavenging activity [30]. Assay for determination of reducing power was performed as per the procedure reported by Oyazi with minor changes [31].

4.4. In vitro study

4.4.1. MTT assay

Antiproliferative potentials and cell cytotoxicity of synthesized compounds were determined by MTT assay as reported earlier [32,33]. Briefly, viable HepG-2, MCF-7 and HEK293 cells were seeded in a 96-well plate (approximately 5×10^3 cells/well). Cancer cell lines were treated with increasing concentrations (5–80 μM) and HEK 293 cells with increasing concentrations from 5 μM to 200 μM of synthesized compounds on following day. After 48 h of incubation, mixtures of medium and synthesized compounds were removed and the cells were rinsed twice with freshly prepared phosphate buffer saline (PBS) followed by treatment with 20 μl MTT (from 5 mg/ml stock). 100 μl DMEM was added into each well and the plate was further incubated for at 37 °C for next 4–5 h in a CO_2 incubator. At last, the residual MTT and medium were removed and the formazan crystals were dissolved in 100 μl DMSO. The plates were shaken for 15–20 min further. Absorbance was recorded at 570 nm using titerplate reader (BioRad). The absorbance values thus measured were converted to percentage viability as compared to the control cells. Camptothecin was taken as positive control for anticancer activities. Selectivity index (SI) values were calculated as described previously [33].

4.4.2. Cell nuclear morphology assay

For cell nuclear morphology study, DAPI (4′,6-diamidino-2-phenylindole) staining technique was performed by following the standard protocol reported previously [33]. In brief, HeLa cells treated with synthesized compounds (**4b, 4d** and **4e)** at their IC_{50} concentrations were incubated for 48 h at 37 °C while control cells were contained only media. After incubation, the cells were rinsed with buffer (PBS), fixed using 70% ethanol and suspended again in 40 μl of DAPI followed by incubation at 37 °C for next 25 min covered. The cells were viewed under fluorescence microscope.

4.4.3. Cell migration assay

As per the standard reported procedure in literature, cell migration assay was carried out [33]. HeLa cells were seeded in a 12-well plate, incubated at 37 °C for 24 h, treated with synthesized compounds (**4b, 4d and 4e**) at IC_{50} concentrations and incubated again for 48 h at 37 °C. Control cells were treated with the media only. After incubation, a wound was made by scratching with pipette tip and placed again in CO_2 incubator. The percentage of healing of wound was calculated and snapped post 48 h incubation. Image J tool was used to add scale bars to images.

4.4.4. Cell cycle analysis

For the study of cell cycle arrest and regulation, flow cytometry was performed according to the standard procedures reported in literature [34,35]. Effects on cell cycle of HeLa cell lines at IC_{50} concentrations of synthesized compounds (**4b, 4d** and **4e)** were analyzed by flow cytometry. On completion of 80% culture area, cells were starved overnight and treated with synthesized compounds (**4b, 4d** and **4e)** for 48 h in complete medium. Later, cells were trypsinised, washed with chilled buffer (PBS) and centrifuged for next 5 min. Further, 800 μl chilled 70% ethanol was added drop wise to the cell pellet with slow mixing followed by incubation at 4 °C for 2 h. It was treated with 20 mg/mL of RNase successively, and the mixture was again incubated at 37 °C for 45 min. The cells were resuspended in 500 μl PBS, Propidium iodide (50 mg/mL) was added and further incubated for 20 min. Flow cytometry was then carried out for cell cycle phase distribution analysis using FACS (Becton Dickinson FACSCaliber System).

4.5. Top1 inhibition assay

The inhibition of potential of synthesized test compounds to Top1 was determined by assessing the relaxation of supercoiled pBR322 plasmid DNA [36]. The assay was carried out in a final volume of 20 μl reaction volume containing 2 μl of 10 × Top1 reaction buffer, 2 μl supercoiled plasmid DNA pBR322 (Takara Biotechnology, Japan), 10 μl of Top1, 6 μl water, 2 μl test compound, 2 μl DNA loading dye. After incubation of reaction mixtures at 37 °C for 30 min, electrophoresis was

done on a 0.8% agarose gel at a potential 90 V for 55 min using 1X TAE buffer. The 5 wells of agarose gel were loaded with supercoiled DNA plasmid, Plasmid and Top1 enzyme, Camptothecin and test compounds (**4b, 4d** and **4e**) respectively. After electrophoresis, the gel was stained with ethidium bromide for 10 min and washed with water for 5 min. The DNA bands were visualized using BioRAD illuminator.

4.6. Molecular docking study

Molecular docking study was carried out to establish different interactions between the test compounds and the target protein [37]. Molecular docking study was performed using the 3D structure of Top1 protein on Maestro 10.5 program (Schrodinger Inc. USA) by 64 bit operating system [Intel (R) Core (TM) i5-2400 CPU @ 2.40 GHz, 6 GB RAM]. The X-ray crystal structure of Human DNA Top1 enzyme forming complex with the known inhibitor Camptothecin (PDB ID: 1T8I) [38] was retrieved from the Protein Data Bank for the present study. The protein obtained was first prepared using protein preparation wizard module. Water molecules and all other undesirable residues were removed other than unique ligand after preprocessing. It was then subjected to hydrogen bond optimization followed by energy minimization. The active site was generated as grid box using Glide. Structure of ligand molecules were drawn as mol file using ChemDraw 12.0 software and their energy was minimized using LigPrep module of Maestro. All possible ionization states at pH 7.0 ± 2.0 were generated and minimized. Ligand molecules prepared were docked into the active site in extra precision mode (XP) using Glide. Docking of compound **4b, 4d** and **4e** into the active site of Human Top1 exhibited several molecular interactions (hydrogen bond, pi-pi interaction and hydrophobic interaction) and were considered to be responsible for the observed activity of the compounds.

4.7. Statistical analysis

Effects were presented as mean value ± SD ($n = 3$). Regression evaluation was performed to find the dose response relation among the synthesized compounds (**4b, 4d** and **4e**). Linear regression was performed to get correlation coefficient. Student's *t*-test was used to determine Significance and a value of $p < 0.05$ was considered to be significant.

Acknowledgments

One of the Research Scholar (RH) is thankful to UGC, Government of India, for providing timely Maulana Azad National Fellowship financial assistance [F1-17.1/2014-15/MANF-2014-15-MUS-BIH-38609] and the other author (KA) is thankful to Indian council of medical research (ICMR), India, for award of Research Associateship [No-3/2/3/16/2018/Online Onco Fship/NCDIII].

Conflict of Interests

The authors confirm that this article contents have no conflicts of interest.

Appendix A. Supplementary data

Supplementary data to this article can be found online at https://doi.org/10.1016/j.bioorg.2019.102962.

References:

[1] L.A. Torre, F. Bray, R.L. Siegel, J. Ferlay, J. Lortet-Tieulent, A. Jemal, Global cancer statistics, CA: Cancer J. Clinicians 65 (2) (2015) 87–108.
[2] A.T. Wong, M. Shao, J. Rineer, V. Osborn, D. Schwartz, D. Schreiber, Treatment and survival outcomes of small cell carcinoma of the esophagus: an analysis of the National Cancer Data Base, Dis. Esophagus: Off. J. Int. Soc. Dis. Esophagus 30 (2) (2017) 1–5.
[3] E. Lacivita, R. Perrone, L. Margari, M. Leopoldo, Targets for drug therapy for autism spectrum disorder: challenges and future directions, J. Med. Chem. 60 (22) (2017) 9114–9141.
[4] B. Stewart, C.P. Wild, World cancer report 2014, 2014.
[5] R.J. Deberardinis, J.J. Lum, G. Hatzivassiliou, C.B. Thompson, The biology of cancer: metabolic reprogramming fuels cell growth and proliferation, Cell Metab. 7 (1) (2008) 11–20.
[6] P. Samadder, R. Aithal, O. Belan, L. Krejci, Cancer TARGETases: DSB repair as a pharmacological target, Pharmacol. Therap. 161 (2016) 111–131.
[7] K. Bandyopadhyay, R.A. Gjerset, Protein kinase CK2 is a central regulator of topoisomerase I hyperphosphorylation and camptothecin sensitivity in cancer cell lines, Biochemistry 50 (5) (2011) 704–714.
[8] M. Sander, T.J. Slaga, B.F. Trump, C.C. Harris, The twenty-second aspen cancer conference: Mechanisms of toxicity, carcinogenesis, cancer prevention, and cancer therapy, 2007, Mol. Carcinog. 47 (7) (2008) 554–571 Published in cooperation with the University of Texas MD Anderson Cancer Center.
[9] K. Bandyopadhyay, C. Lee, A. Haghighi, J.-L. Banères, J. Parello, R.A. Gjerset, Serine phosphorylation-dependent coregulation of topoisomerase I by the p14ARF tumor suppressor, Biochemistry 46 (49) (2007) 14325–14334.
[10] R.P. Bender, N. Osheroff, 3 DNA Topoisomerases, Checkpoint Responses Cancer Therapy (2008) 57.
[11] R. Bermejo, Y. Doksani, T. Capra, Y.-M. Katou, H. Tanaka, K. Shirahige, M. Foiani, Top1-and Top2-mediated topological transitions at replication forks ensure fork progression and stability and prevent DNA damage checkpoint activation, Genes Dev. 21 (15) (2007) 1921–1936.
[12] Y. Pommier, Y. Sun, N.H. Shar-yin, J.L. Nitiss, Roles of eukaryotic topoisomerases in transcription, replication and genomic stability, Nat. Rev. Mol. Cell Biol. 17 (11) (2016) 703.
[13] K. Cheng, N.J. Rahier, B.M. Eisenhauer, R. Gao, S. Thomas, S.M. Hecht, 14-Azacamptothecin: a potent water-soluble topoisomerase I poison, J. Am. Chem. Soc. 127 (3) (2005) 838–839.
[14] B.L. Staker, M.D. Feese, M. Cushman, Y. Pommier, D. Zembower, L. Stewart, A.B. Burgin, Structures of three classes of anticancer agents bound to the human topoisomerase I− DNA covalent complex, J. Med. Chem. 48 (7) (2005) 2336–2345.
[15] E. Marco, W. Laine, C. Tardy, A. Lansiaux, M. Iwao, F. Ishibashi, C. Bailly, F. Gago, Molecular determinants of topoisomerase I poisoning by lamellarins: comparison with camptothecin and structure − activity relationships, J. Med. Chem. 48 (11) (2005) 3796–3807.
[16] M. Cushman, M. Jayaraman, J.A. Vroman, A.K. Fukunaga, B.M. Fox, G. Kohlhagen, D. Strumberg, Y. Pommier, Synthesis of new indeno [1, 2-c] isoquinolines: cytotoxic non-camptothecin topoisomerase I inhibitors, J. Med. Chem. 43 (20) (2000) 3688–3698.
[17] B. Zhang, X. Li, B. Li, C. Gao, Y. Jiang, Acridine and its derivatives: a patent review (2009–2013), Expert Opin. Therap. Patents 24 (6) (2014) 647–664.
[18] M. Wainwright, Acridine—a neglected antibacterial chromophore, J. Antimicrob. Chemother. 47 (1) (2001) 1–13.
[19] A. Chilin, G. Marzaro, C. Marzano, L. Dalla Via, M.G. Ferlin, G. Pastorini, A. Guiotto, Synthesis and antitumor activity of novel amsacrine analogs: the critical role of the acridine moiety in determining their biological activity, Bioorg. Med. Chem. 17 (2) (2009) 523–529.
[20] F. Charmantray, A. Martelli, Interest of acridine derivatives in the anticancer chemotherapy, Curr. Pharm. Des. 7 (17) (2001) 1703–1724.
[21] A.F.-C. Valdés, Acridine and acridinones: old and new structures with antimalarial activity, Open Med. Chem. J. 5 (2011) 11.
[22] J.R. Goodell, A.A. Madhok, H. Hiasa, D.M. Ferguson, Synthesis and evaluation of acridine-and acridone-based anti-herpes agents with topoisomerase activity, Bioorg. Med. Chem. 14 (16) (2006) 5467–5480.
[23] R. Munawar, N. Mushtaq, S. Arif, A. Ahmed, S. Akhtar, S. Ansari, S. Meer, Z.S. Saify, M. Arif, Synthesis of 9-aminoacridine Derivatives as Anti-alzheimer Agents, Am. J. Alzheimer's Dis. Other Dementias® 31 (3) (2016) 263–269.
[24] C.H. Allen, G.H.W McKee, Org. Synth 19 (1939) 6–9.
[25] A. Albert, B. Ritchie, 9-Aminoacridine: Acridine, 9-amino-, Org. Synth. 22 (2003) 5.
[26] D. Pearson, K. Carter, C. Greer, The rearrangement of hydrazones and semicarbazones, J. Am. Chem. Soc. 75 (23) (1953) 5905–5908.
[27] G. Miliauskas, P. Venskutonis, T. Van Beek, Screening of radical scavenging activity of some medicinal and aromatic plant extracts, Food Chem. 85 (2) (2004) 231–237.
[28] F. Liu, V. Ooi, S. Chang, Free radical scavenging activities of mushroom polysaccharide extracts, Life Sci. 60 (10) (1997) 763–771.
[29] R.J. Ruch, S.-J. Cheng, J.E. Klaunig, Prevention of cytotoxicity and inhibition of intercellular communication by antioxidant catechins isolated from Chinese green tea, Carcinogenesis 10 (6) (1989) 1003–1008.
[30] L.C. Green, D.A. Wagner, J. Glogowski, P.L. Skipper, J.S. Wishnok, S.R. Tannenbaum, Analysis of nitrate, nitrite, and [15N]nitrate in biological fluids, Anal. Biochem. 126 (1) (1982) 131–138.
[31] M. Oyaizu, Studies on products of browning reaction: antioxidative activities of products of browning reaction prepared from glucosamine, Jpn. J. Nutr. (44) (1986) 307–315.
[32] M.F. Ansari, S.M. Siddiqui, K. Ahmad, F. Avecilla, S. Dharavath, S. Gourinath, A. Azam, Synthesis, antiamoebic and molecular docking studies of furan-thiazolidinone hybrids, Eur. J. Med. Chem. 124 (2016) 393–406.
[33] R. Khanam, K. Ahmad, I.A. Hejazi II, V. Siddique, A.R. Kumar, A. Bhat, F. Athar Azam, Inhibitory growth evaluation and apoptosis induction in MCF-7 cancer cells by new 5-aryl-2-butylthio-1,3,4-oxadiazole derivatives, Cancer Chemother. Pharmacol. 80 (5) (2017) 1027–1042.

[34] S.R. Jayapal, C.Q. Wang, X. Bisteau, M.J. Caldez, S. Lim, V. Tergaonkar, M. Osato, P. Kaldis, Hematopoiesis specific loss of Cdk2 and Cdk4 results in increased erythrocyte size and delayed platelet recovery following stress, Haematologica 100 (4) (2015) 431–438.
[35] W.-W. Lai, J.-S. Yang, K.-C. Lai, C.-L. Kuo, C.-K. Hsu, C.-K. Wang, C.-Y. Chang, J.-J. Lin, N.-Y. Tang, P.-Y. Chen, Rhein induced apoptosis through the endoplasmic reticulum stress, caspase-and mitochondria-dependent pathways in SCC-4 human tongue squamous cancer cells, Vivo 23 (2) (2009) 309–316.
[36] R. Chaniyara, S. Tala, C.-W. Chen, X. Zang, R. Kakadiya, L.-F. Lin, C.-H. Chen, S.-I. Chien, T.-C. Chou, T.-H. Tsai, Novel antitumor indolizino [6, 7-b] indoles with multiple modes of action: DNA cross-linking and topoisomerase I and II inhibition, J. Med. Chem. 56 (4) (2013) 1544–1563.
[37] J. Akhtar, A.A. Khan, Z. Ali, R. Haider, M.S. Yar, Structure-activity relationship (SAR) study and design strategies of nitrogen-containing heterocyclic moieties for their anticancer activities, Eur. J. Med. Chem. 125 (2017) 143–189.
[38] R. Badisa, L. Ayuk-Takem, C. Ikediobi, E. Walker, Selective anticancer activity of pure licamichauxiioic-B acid in cultured cell lines, Pharm. Biol. 44 (2) (2006) 141–145.
[39] M. Li, Y. Liu, Topoisomerase I in human disease pathogenesis and treatments, Genom. Proteom. Bioinformatics 14 (3) (2016) 166–171.
[40] D. Wu, D.-W. Zhao, Y.-Q. Li, W.-G. Shi, Q.-L. Yin, Z.-K. Tu, Y.-Y. Yu, B.-H. Zhong, H. Yu, W.-G. Bao, Antitumor potential of a novel camptothecin derivative, ZBH-ZM-06, Oncol. Rep. 39 (2) (2018) 871–879.
[41] V. Zaharia, A. Ignat, B. Ngameni, V. Kuete, M.L. Moungang, C.N. Fokunang, M. Vasilescu, N. Palibroda, C. Cristea, L. Silaghi-Dumitrescu, B.T. Ngadjui, Heterocycles 23: synthesis, characterization and anticancer activity of new hydrazinoselenazole derivatives, Med. Chem. Res. 22 (12) (2013) 5670–5679.
[42] M. Varache-Lembège, S. Moreau, S. Larrouture, D. Montaudon, J. Robert, A. Nuhrich, Synthesis and antiproliferative activity of aryl-and heteroaryl-hydrazones derived from xanthone carbaldehydes, Eur. J. Med. Chem. 43 (6) (2008) 1336–1343.